Molecularly Imprinted Polymers

International Edition: DOI: 10.1002/anie.201805772
German Edition: DOI: 10.1002/ange.201805772

Highly Efficient Synthesis and Assay of Protein-Imprinted Nanogels by Using Magnetic Templates

*Rashmi Mahajan[+], Mona Rouhi[+], Sudhirkumar Shinde, Thomas Bedwell, Anil Incel, Liliia Mavliutova, Sergey Piletsky, Ian A. Nicholls, and Börje Sellergren**

Abstract: *We report an approach integrating the synthesis of protein-imprinted nanogels ("plastic antibodies") with a highly sensitive assay employing templates attached to magnetic carriers. The enzymes trypsin and pepsin were immobilized on amino-functionalized solgel-coated magnetic nanoparticles (magNPs). Lightly crosslinked fluorescently doped polyacrylamide nanogels were subsequently produced by high-dilution polymerization of monomers in the presence of the magNPs. The nanogels were characterised by a novel competitive fluorescence assay employing identical protein-conjugated nanoparticles as ligands to reversibly immobilize the corresponding nanogels. Both nanogels exhibited $K_d < 10$ pM for their respective target protein and low cross-reactivity with five reference proteins. This agrees with affinities reported for solid-phase-synthesized nanogels prepared using low-surface-area glass-bead supports. This approach simplifies the development and production of plastic antibodies and offers direct access to a practical bioassay.*

Molecular imprinting refers to a templating technique for producing molecular recognition sites in synthetic network polymers. This approach has been used to generate porous materials or nanoparticles exhibiting receptor-like affinity for a large variety of template structures.[1–6] Commonly referred to as plastic antibodies, these can now be produced featuring binding properties resembling those of antibodies and of a size comparable to large proteins (e.g., IgM).[7] Their ability to function in complex environments including biofluids in vivo has considerably expanded their scope of applications, mainly as antibody substitutes in assays, sensors, separations, probes, and drugs or drug delivery vehicles compatible with in vivo applications. The development of new and improved methods for producing and characterising these receptors and methods for integrating them into practical bioassays are urgently needed to translate the research results to practical applications.

Nanoparticles or nanogels can be produced by precipitation or emulsion polymerization, or grafting of polymers from preformed core particles.[8–12] These feature the characteristic properties of nanosized objects, that is, high specific surface area, fast mass transfer, and susceptibility to aggregation. Furthermore, by reducing the size of the molecularly imprinted polymer (MIP) to form particles in the nanometer range, MIPs with on average one site per particle can be produced.[13] Heterogeneity is due to the non-equivalence of sites between the particles (see, for example, polyclonal antibodies) and as polyclonal antibodies the particles can be fractionated and enriched by affinity chromatography. Such soluble MIPs are more difficult to process in terms of template removal and binding tests, which typically require lengthy protocols of repeated wash/centrifugation or dialysis steps.[7]

An elegant approach overcoming these limitations is surface imprinting of nanoparticles by solid-phase synthesis.[14,15] The nanoparticles are synthesized in presence of template-modified solid supports whereby growing particles adhere to the support surface. Post-synthesis, the particles can be affinity-purified in situ leading to high affinity receptors in template-free form. A limitation with the examples demonstrated thus far is related to the low specific surface area of the solid-support beads. This translates into low particle yields (< 1 mg g^{-1} support beads) and a need for large reactors, which essentially limits the technique to serial synthesis protocols. To overcome this limitation, we recently introduced a scalable process to produce surface-imprinted nanoparticles in high yield and in template-free form.[16] The approach is based on the use of nanosized magnetic template carriers (Figure 1) in a process tolerating high template concentrations. In a first proof-of-concept demonstration, we used a non-aqueous small-molecule-imprinting protocol to isolate circa 17 mg of imprinted particles from only 50 mg of magnetic carrier. This is equal to a yield of 340 mg MIP per gram of carrier, making the method compatible with both

[*] M. Rouhi,[+] S. Shinde, A. Incel, L. Mavliutova, B. Sellergren
Department of Biomedical Sciences and Biofilms-Research Center for Biointerfaces (BRCB), Faculty of Health and Society
Malmö University
205 06 Malmö (Sweden)
E-mail: borje.sellergren@mau.se
R. Mahajan,[+] I. A. Nicholls
Bioorganic and Biophysical Chemistry Laboratory, Linnaeus University Centre for Biomaterials Chemistry, Department of Chemistry and Biomedical Sciences, Linnaeus University
391 82 Kalmar (Sweden)
T. Bedwell, S. Piletsky
Chemistry Department, College of Science and Engineering
University of Leicester
Leicester, LE1 7RH (UK)
[+] These authors contributed equally to this work.
Supporting information and the ORCID identification number(s) for the author(s) of this article can be found under: https://doi.org/10.1002/anie.201805772.

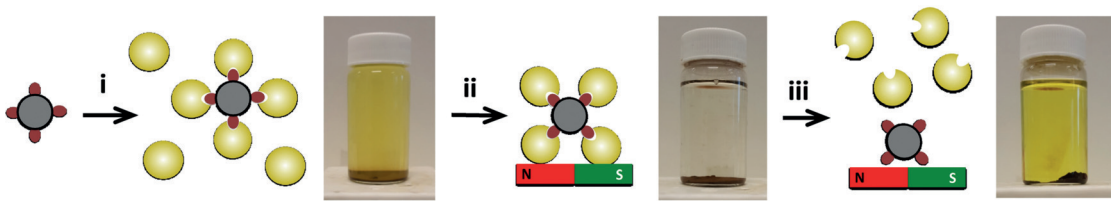

Figure 1. Principle of using magnetic templates for synthesis, affinity enrichment, and purification of FITC-labeled protein-imprinted nanogels and images of a reaction vessel (P-NG) during the process. i) Polymerization of acrylamide monomers, ii) magnetic collection and removal of unreacted monomers by rinsing, and iii) heat-induced (60 °C) release of imprinted nanogel leading to enrichment of high-affinity imprinted nanogel.

small-scale parallel synthesis and large-scale synthesis by established polymerization techniques.

A technique that is rapidly gaining in importance is the high-dilution polymerization of acrylamide monomers to produce imprinted nanogels.[7,15,17,18] With a nearly generic synthesis protocol, plastic antibodies can be prepared featuring both size and affinity in the range of those of native antibodies. We demonstrate that the magnetic template technique can be used to cut time and significantly boost the yield of nanogels in this protocol. We moreover demonstrate a generic approach integrating synthesis and a practical binding assay using the same magnetic templates.

Magnetite was chosen as a magnetic core, since this material can be obtained conveniently by the co-precipitation of Fe^{II}/Fe^{III} in aqueous media under base catalysis. A silica shell was then applied by aqueous hydrolysis of tetraethyl orthosilicate (TEOS) in glycerol followed by amino-functionalization with APTMS and glutaraldehyde-based coupling of the templates, that is, the proteolytic enzymes trypsin and pepsin (Supporting Information, Figure S1).

Trypsin (23 kDa, pI = 10) and pepsin (35 kDa, pI = 2–3) are thermally stable oppositely charged proteolytic enzymes that have been previously used as model templates to produce high-affinity nanogels.[18] The resulting magnetic nanoparticles (magNPs) were characterised by dynamic light scattering (DLS), FTIR spectroscopy, and TEM. TEM images (Figure 2A) revealed irregularly shaped agglomerates of core particles, with an average size according to DLS of 200 nm and a polydispersity of 0.2–0.3 (Table 1, Figure 2A, and Figure S2). The presence of immobilized protein is indicated by the appearance of the characteristic amide stretching bands at 1653 cm^{-1} and 1487 cm^{-1} (Figure S3). Thermal gravimetric analysis (TGA) mass-loss curves showed an excessive mass loss of circa 6% and 9% for the pepsin- and trypsin-modified particles (Figure S4) in agreement with the relative IR band intensities. This corresponds to a coupling yield of 1.7 and 3.9 μmol g^{-1}, respectively, translating into a surface coverage of 0.015 and 0.035 μmol m^{-2}, respectively, assuming a specific surface area of 110 $m^2 g^{-1}$. This is comparable to the surface coverage used in the glass-bead approach.[18] The measured zeta-potentials furthermore agreed with the nature of the surface functionalizations.

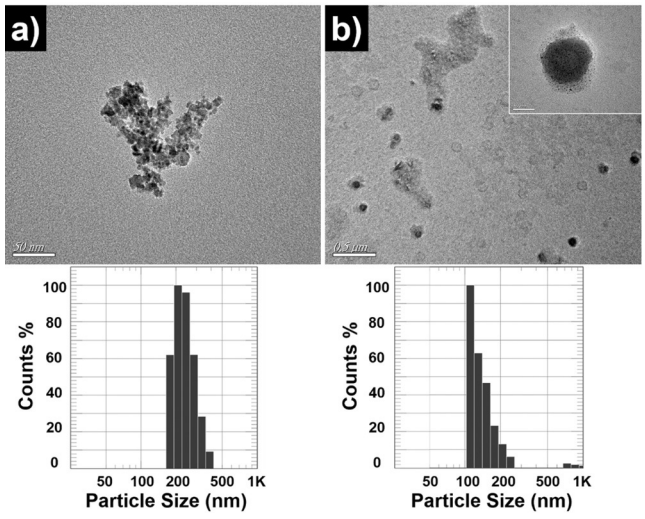

Figure 2. DLS plots (water, bottom) and TEM images (top) of A) magNP-NH_2 and B) T-NG. Scale bar = 50 nm (a), 500 nm (b), and 50 nm (inset).

The template-modified magnetic particles (50 mg) were introduced in place of free soluble protein or protein-modified glass beads used in the previously established nanogel-imprinting protocols.[7,15] The monomers used in the latter include *N*-isopropylacrylamide (NIPAm) as backbone monomer and *N*,*N*′methylenebisacrylamide (BIS) as cross-linker in combination with *N*-*t*-butylacrylamide (TBAm), acrylic acid (AA), and aminopropylmethacrylamide (APMA), the latter three added to balance hydrophobic, cationic, and anionic sites on the protein surface, respectively.

Fluorescent tracking of the nanogel particles was enabled by addition of a small amount of *N*-fluoresceinylacrylamide. The monomers (C_{tot} = 6.5 mM) were dissolved in 50 mL of water and the polymerization was initiated using the redox couple ammonium persulfate (APS) and *N*,*N*,*N*′,*N*′-tetramethylethylenediamine (TEMED) and allowed to proceed overnight at room temperature. It was assumed that polymer chains growing in contact with the protein template would remain multivalently attached and that these could be isolated by magnetic collection followed by heat- or solvent-induced elution (Figure 1). In this approach, polymerization occurs in a nanoparticle dispersion contrasting with the previously introduced approach for solid-phase synthesis.[18] The anticipated interactions were supported by DLS and TEM results for independently synthesized particle batches. DLS showed a circa 130 nm increase in size after mixing P-NG and magNP-P (Figure S5).

To assess the extent of firmly attached nanogel particles, the magNPs were washed with water followed by heat-induced elution of firmly bound particles.[15] The three fractions, that is, the crude reaction mixture, the wash

fraction, and the elution fraction, are seen in Figure 1. The yellow color indicates the presence of the FITC dye used to label the nanogel particles. The intense color in the crude reaction mixture reveals the presence of a significant amount of non-attached polymer or unreacted monomer. This fraction is removed by magnetic collection. The final wash fraction is nearly clear showing that the amount of labelled particles released in this step is small. This contrasts with the intense yellow color shown in the elution step, reflecting the release of a significant quantity of labelled polymer. The mass of eluted polymer was determined gravimetrically on freeze-dried (or dried) fractions. This consistently showed that approximately 10 mg of polymer could be recovered in the elution step, translating into a conversion of monomer into particle-attached nanogel of circa 13% based on added monomer. This moreover corresponds to a stock nanogel concentration of circa 0.1 mg mL^{-1}. The hydrodynamic size and dry morphology of the particles were characterised by DLS and TEM (Figure 2B). DLS revealed the presence of circa 130 nm particles with a polydispersity of 0.7–1 and a negative zeta-potential (Table 1, Figure 2B, and Figures S5 and S6). This size agreed with the TEM analysis.

We next turned to the binding tests and assay format. In our previous report we used a colorimetric test to detect unbound nanoparticles in presence of template-modified magNPs.[16] Given the FITC-label incorporated in the nanogels, we likewise thought that fluorescence detection could be used to establish a competitive displacement assay (Figure 3). In order to test this approach, we first investigated the nanogel fluorescence emission intensity ($\lambda_{ex} = 485$ nm, $\lambda_{em} = 520$ nm) in response to added proteins in solution (Figure S7). No significant change in emission intensity or maximum was observed when adding proteins in the concentration range 0.1 nM–1 μM.

We then incubated 100 μL of the nanogel stock solution with magNP-T or magNP-P and transferred the mixture to the wells of a 96-well plate equipped with magnetic ring-shaped insets leaving the center of the well open for optional fluorescence reading from either bottom or top. Figure 4A shows the emission spectra of the trypsin nanogel (T-NG) in absence or presence of magNP-T, the magNP-T alone, and the mixture after addition of trypsin or pepsin. Interestingly, the emission intensity was significantly higher after addition of the template protein. Conversely, using magNP-P and P-NG (Figure 4B) resulted in the same behaviour but now with the largest intensity increase being observed when adding pepsin.

We then turned to a more extensive investigation of the displacement effect for a wider concentration interval and in response to equilibration time. The result is seen in Figure S8. After a 30 min equilibration time, the difference in signal intensity in response to added protein (T or P) is relatively small (< 20% of total intensity). This contrasts with the results obtained after a 2 h equilibration. The intensity measured when adding trypsin to the magNP-T–T-NG complex (Figure 4C) or pepsin to magNP-P–P-NG (Figure 4D), was 2–3-fold higher than when adding noncomplementary hard and soft proteins of different sizes and charges (Table S1).

The effect was observed for concentrations as low as 10 pM indicating dissociation constants in the picomolar range, in agreement with previous literature reports describing solid-phase (glass bead) synthesised nanogels. The slow equilibration possibly reflects the involvement of multivalent interactions between the nanogels and the magNPs. A similar response was recorded in the presence of an excess of albumin (Figure S9) indicating compatibility of the assay with more complex matrices.

The reported synthesis method profits from the high surface-to-volume ratio of template-decorated magnetic nanoparticles resulting in a considerably higher product yield of affinity-enriched imprinted particles compared to the established glass-bead approach. These same components can then be directly used in a practical fluorescence-based competitive displacement assay featuring sensitivity on the order of traditional ELISAs while obviating the need for ligand or nanogel immobilizations or enzyme conjugations. This integrated approach simplifies in a major way the development and production of plastic antibodies and offers direct access to a practical bioassay.

Table 1: Zeta-potential, average particle size, and dispersity (*Đ*) from DLS of nanoparticles used in the study.

Particle[a]	Diameter (nm)	*Đ*	Zeta-potential	Mass loss (%)[c]
magNP	227	0.226	−8.22	4.7
magNP@SiO_2	280	0.216	−17.78	5.6
magNP-NH_2	331	0.151	1.22	5.7
magNP-T	462	0.261	−10.98	14.6
magNP-P	403	0.298	−1.67	11.3
T-NG[b]	139	1.037	−35	–
P-NG[b]	125	0.714	−34	–

[a] DLS was performed using water as dispersing solvent. [b] The gravimetric yields were 8 mg for T-NG and 10 mg for P-NG. [c] Mass loss in the interval 120 °C–800 °C.

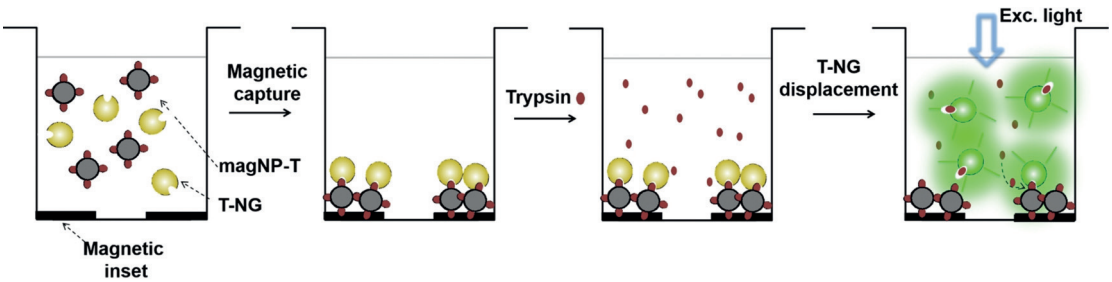

Figure 3. Principle of the magnetic template-based displacement assay.

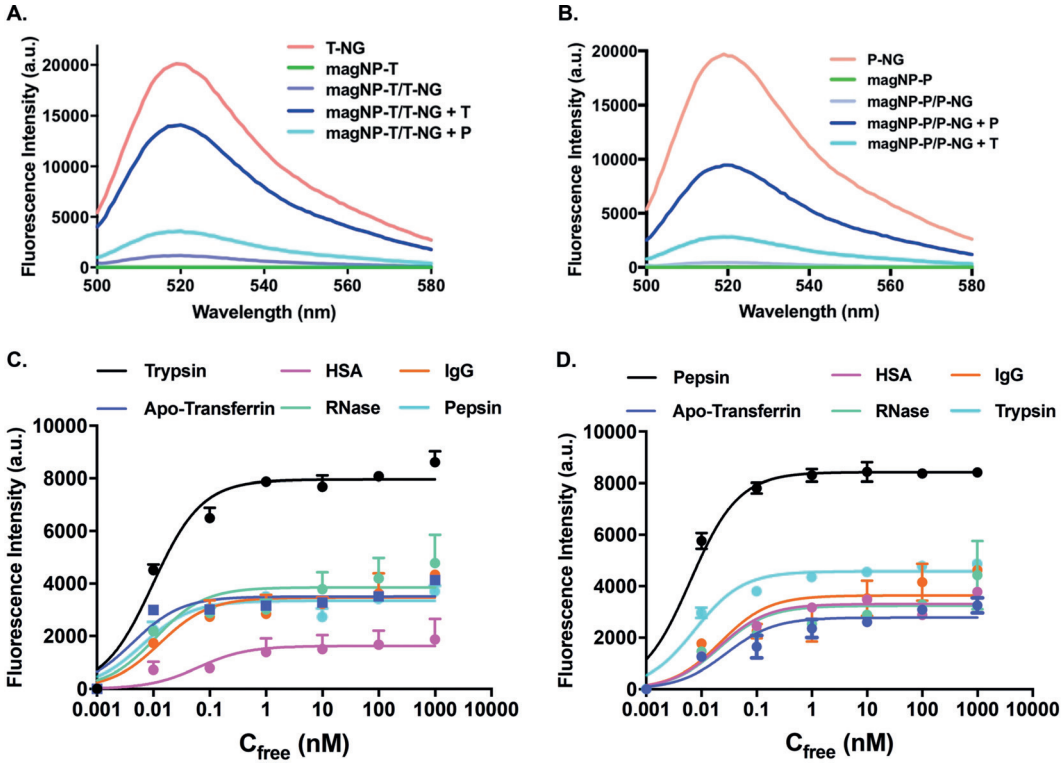

Figure 4. Fluorescence spectra of A) magNP-T, T-NG, magNP-T/T-NG, magNP-T/T-NG + trypsin, and magNP-T/T-NG + pepsin. Fluorescence spectra of B) magNP-P, P-NG, magNP-P/P-NG, magNP-P/P-NG + pepsin, and magNP-P/P-NG + trypsin. Fluorescence intensity of displaced nanogel C) T-NG or D) P-NG immobilized on the corresponding magNPs upon addition of incremental amounts of different proteins and incubation for 2 h. The excitation/emission filters used were 485/520 nm.

Acknowledgements

We acknowledge financial support from the Marie Skłodowska-Curie Actions (H2020-MSCA-ITN-2016, 722171—Biocapture) and the Sweden Knowledge-Foundation for research under Synergi grant number 20150086. I.A.N acknowledges financial support from Sweden Knowledge Foundation for research under BIO-QC, grant number 20170059 and from Vetenskapsrådet VR under grant number 2014-4573.

Conflict of interest

The authors declare no conflict of interest.

Keywords: competitive assays · molecularly imprinted polymers · nanogel synthesis · plastic antibodies

How to cite: *Angew. Chem. Int. Ed.* **2019**, *58*, 727 – 730
Angew. Chem. **2019**, *131*, 737 – 740

[1] M. J. Whitcombe, N. Kirsch, I. A. Nicholls, *J. Mol. Recognit.* **2014**, *27*, 297 – 401.
[2] L. Chen, X. Wang, W. Lu, X. Wu, J. Li, *Chem. Soc. Rev.* **2016**, *45*, 2137 – 2211.
[3] K. Haupt, C. Ayela, *Molecular Imprinting*, Springer, Berlin, **2012**.
[4] B. Sellergren, A. J. Hall, in *Supramolecular Chemistry: from Molecules to Nanomaterials* (Eds.: J. W. Steed, P. A. Gale), Wiley, Chichester, **2012**, pp. 3255 – 3282.
[5] T. Takeuchi, T. Hayashi, S. Ichikawa, A. Kaji, M. Masui, H. Matsumoto, R. Sasao, *Chromatography* **2016**, *37*, 43 – 64.
[6] W. J. Cheong, S. H. Yang, F. Ali, *J. Sep. Sci.* **2013**, *36*, 609 – 628.
[7] Y. Hoshino, T. Kodama, Y. Okahata, K. J. Shea, *J. Am. Chem. Soc.* **2008**, *130*, 15242 – 15243.
[8] J. Wang, A. G. Cormack, P. C. Sherrington, D. E. Khoshdel, *Angew. Chem. Int. Ed.* **2003**, *42*, 5336 – 5338; *Angew. Chem.* **2003**, *115*, 5494 – 5496.
[9] D. Vaihinger, K. Landfester, I. Krauter, H. Brunner, G. E. M. Tovar, *Macromol. Chem. Phys.* **2002**, *203*, 1965 – 1973.
[10] C. Li, B. C. Benicewicz, *Macromolecules* **2005**, *38*, 5929 – 5936.
[11] G. Pan, Y. Zhang, Y. Ma, C. Li, H. Zhang, *Angew. Chem. Int. Ed.* **2011**, *50*, 11731 – 11734; *Angew. Chem.* **2011**, *123*, 11935 – 11938.
[12] Y. Hoshino, H. Koide, T. Urakami, H. Kanazawa, T. Kodama, N. Oku, K. J. Shea, *J. Am. Chem. Soc.* **2010**, *132*, 6644 – 6645.
[13] G. Wulff, B.-O. Chong, U. Kolb, *Angew. Chem. Int. Ed.* **2006**, *45*, 2955 – 2958; *Angew. Chem.* **2006**, *118*, 3021 – 3024.
[14] A. Poma, A. Guerreiro, M. J. Whitcombe, E. V. Piletska, A. P. F. Turner, S. A. Piletsky, *Adv. Funct. Mater.* **2013**, *23*, 2821 – 2827.
[15] F. Canfarotta, A. Poma, A. Guerreiro, S. Piletsky, *Nat. Protoc.* **2016**, *11*, 443.
[16] M. Berghaus, R. Mohammadi, B. Sellergren, *Chem. Commun.* **2014**, *50*, 8993 – 8996.
[17] S. Ambrosini, S. Beyazit, K. Haupt, B. Tse Sum Bui, *Chem. Commun.* **2013**, *49*, 6746 – 6748.
[18] A. Guerreiro, A. Poma, K. Karim, E. Moczko, J. Takarada, I. Perez de Vargas-Sansalvador, N. Turner, E. Piletska, C. Schmidt de Magalhães, N. Glazova, A. Serkova, A. Omelianova, S. Piletsky, *Adv. Healthcare Mater.* **2014**, *3*, 1426 – 1429.

Manuscript received: May 22, 2018
Revised manuscript received: September 10, 2018
Accepted manuscript online: October 11, 2018
Version of record online: November 15, 2018

